Burgers Turbulence in the Fermi-Pasta-Ulam-Tsingou Chain

Matteo Gallone,[1,*] Matteo Marian,[2,†] Antonio Ponno,[3,‡] and Stefano Ruffo[1,4,5,§]
[1]*SISSA, Via Bonomea 265, 34136 Trieste, Italy*
[2]*Department of Physics, University of Trieste, Via A. Valerio 2, 34127 Trieste, Italy*
[3]*Department of Mathematics "T. Levi-Civita," University of Padova, Via Trieste 63, 35121 Padova, Italy*
[4]*INFN Sezione di Trieste, via Valerio, 2 34127 Trieste, Italy*
[5]*ISC-CNR, via Madonna del Piano 10, 50019 Sesto Fiorentino (Firenze), Italy*

(Received 25 March 2022; revised 12 July 2022; accepted 15 August 2022; published 8 September 2022)

We prove analytically and show numerically that the dynamics of the Fermi-Pasta-Ulam-Tsingou chain is characterized by a transient Burgers turbulence regime on a wide range of time and energy scales. This regime is present at long wavelengths and energy per particle small enough that equipartition is not reached on a fast timescale. In this range, we prove that the driving mechanism to thermalization is the formation of a shock that can be predicted using a pair of generalized Burgers equations. We perform a perturbative calculation at small energy per particle, proving that the energy spectrum of the chain E_k decays as a power law, $E_k \sim k^{-\zeta(t)}$, on an extensive range of wave numbers k. We predict that $\zeta(t)$ takes first the value $8/3$ at the Burgers shock time, and then reaches a value close to 2 within two shock times. The value of the exponent $\zeta = 2$ persists for several shock times before the system eventually relaxes to equipartition. During this wide time window, an exponential cutoff in the spectrum is observed at large k, in agreement with previous results. Such a scenario turns out to be universal, i.e., independent of the parameters characterizing the system and of the initial condition, once time is measured in units of the shock time.

DOI: 10.1103/PhysRevLett.129.114101

Introduction.—Understanding the route to thermalization of an isolated physical system is a fundamental problem in statistical mechanics. The behavior close to equilibrium has been widely understood, while the situation is much more complex when the system is initialized far from equilibrium [1]. Historically, the first system that did not display thermalization on the observation timescale was the Fermi-Pasta-Ulam-Tsingou (FPUT) chain [2,3]. The authors studied, in a computer simulation, a simple one-dimensional model of nonlinearly interacting classical particles with the aim of observing the rate of thermalization. Instead of the expected trend to equilibrium, they observed a "recurrent," quasiperiodic behavior and a lack of energy equipartition among the Fourier modes. An interpretation of such a "FPUT paradox" in terms of Korteweg–de Vries (KdV) solitons was provided in Ref. [4]. A complementary interpretation, based on the so-called Kolmogorov-Arnol'd-Moser theory [5], was proposed in Ref. [6], where the FPUT phenomenon was linked to the criterion of "resonance overlap" for the transition to chaos. The problem of thermalization is still a subject of active investigation: phenomena related to the FPUT recurrence have been observed in several systems, from graphene resonators [7] to nonlinear phononic [8] and photonic [9] systems, from trapped cold atoms [10] to Bose-Einstein condensates [11,12].

The FPUT model consists of N unit masses sitting on a one-dimensional lattice and connected by nearest-neighbor nonlinear springs. The Hamiltonian of the $\alpha + \beta$ FPUT model is

$$H = \sum_{j=1}^{N} \left[\frac{p_j^2}{2} + V(q_{j+1} - q_j) \right], \tag{1}$$

where $V(z) = (z^2/2) + \alpha(z^3/3) + \beta(z^4/4)$, and q_j is the displacement from equilibrium of the jth mass and p_j its momentum.

If the nonlinear part of the interaction vanishes, i.e., $\alpha = \beta = 0$, the dynamics of the Fourier energy spectrum (FES) becomes trivial, since no exchange of energy among the Fourier modes is possible. Thermalization is driven by nonlinearity, which couples the modes causing energy exchange. However, mode coupling takes place also in nonlinear integrable systems, such as the Toda chain [13], where no thermalization occurs. The approach to equilibrium of integrable systems has been studied recently in Ref. [14].

A generic feature of both integrable and quasi-integrable one-dimensional systems is the presence of an exponentially decaying FES [15,16]. Moreover, for the FPUT model, the long wavelength modes form a "packet" of size $\varepsilon^{1/4}$ [17,18], where ε is the specific energy $\varepsilon = E/N$. This scenario describes the behavior of the FES of quasi-integrable systems on timescales increasing as inverse power laws of ε [19,20], whereas for integrable systems

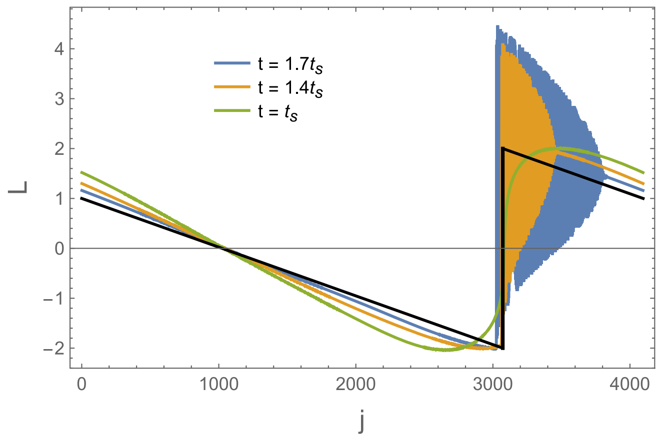

FIG. 1. Numerical simulation of the FPUT model Eq. (1) for $\varepsilon = 0.07$, $N = 4096$, $\alpha = 1$, and $\beta = 1/2$. The colored solid lines are the profiles corresponding to a left traveling wave excitation (TWE) plotted at the shock time t_s, Eq. (7), and at later times. Note the evolution toward a sawtooth profile (black solid line) followed by fast oscillations (discussed in the text).

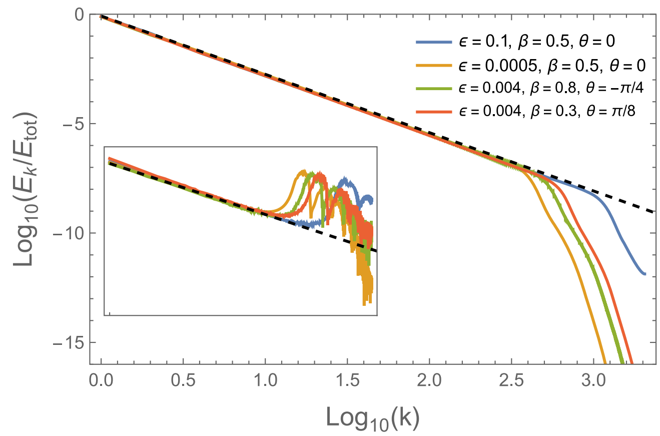

FIG. 2. Normalized FES of the FPUT model Eq. (1) for $\alpha = 1$, different values of β, and $N = 4096$ at the shock time t_s, Eq. (7). The initial condition is given by Eq. (4) with different values of $\theta = \varphi - \pi/4$ and ε. The dashed line is the theoretical prediction given in Eq. (12) $E_k/E \simeq 0.8k^{-8/3}$. Note the exponential cutoff at large k. Inset: FES at $4t_s$ for the same initial conditions. The dashed line is the theoretical prediction $E_k \sim k^{-2}$.

the FES remains exponentially localized for all times. It is known [6] that the FPUT chain relaxes to equipartition on a faster timescale at sufficiently large specific energies [21,22]. More recently, it was shown that relaxation takes place also at smaller energies; see Ref. [20] for a discussion. Relaxation eventually occurs also in the energy range studied in this Letter.

In this Letter, we study the FPUT chain in a regime where the specific energy ε is large enough that mode coupling acts on a wide range of long wavelength modes, but is still small enough to slow down thermalization. In this regime the long wavelength FES turns out to be a scale invariant power law, which motivates the use of the term "turbulence" to describe this phenomenon. The range of involved modes is of the size of the packet quoted above. Our analysis begins with the observation that, in this regime, the time evolution of an initial wave leads to the formation of a "shock," as shown in Fig. 1. This behavior was first described in Ref. [23] and is strongly related to the nondispersive limit of the KdV equation [4,24], i.e., the inviscid Burgers equation. In this Letter, we show that the dynamics of the FPUT chain, in a specific time range, is well described by a pair of *generalized* Burgers equations.

Our approach allows us to derive rigorously and compute analytically some properties of the FES in a wide range of specific energy values.

Main results.—Corresponding to an initial excitation of the longest wavelength, we determine a window of low modes where the FES scales with an inverse time-dependent power law:

$$E_k \sim k^{-\zeta(t)}, \qquad k_0 \leq k \leq k_c, \tag{2}$$

with k_0 and k_c slowly depending on time. The window $[k_0, k_c]$ scales with the number of particles N, i.e., is *extensive* in N, and k_0 is of order 1. We find a shock timescale t_s that characterizes a fast energy transfer from the initially excited mode $k = 1$ to the higher ones. The value of the exponent $\zeta(t)$ at t_s is $\zeta(t_s) = 8/3$, as shown in Fig. 2. We determine analytically both t_s and the corresponding value of the exponent in terms of the underlying Burgers dynamics of the system. We then observe that within a time $\sim 2t_s$, the exponent $\zeta(t)$ decreases to a value of about 2; see Fig. 3 and the inset of Fig. 2. The FES $E_k \sim k^{-2}$ is preserved up to four shock times, after which the power-law structure is lost and the system eventually reaches the statistical equilibrium characterized by an almost flat FES (energy equipartition), as shown in Fig. 3 by the growth of the slope at later times. The whole phenomenology

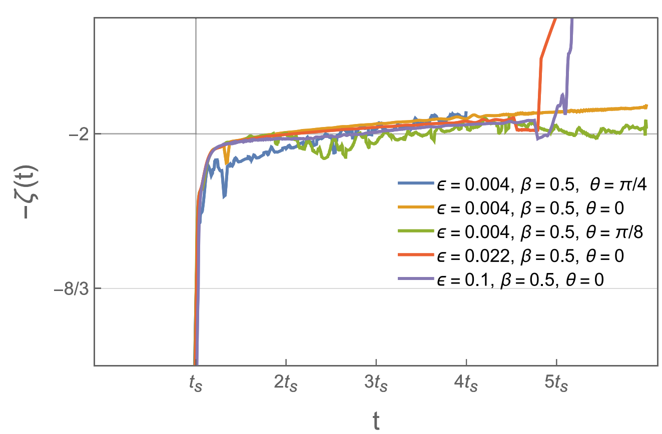

FIG. 3. Slope $-\zeta(t)$ of the power law that interpolates the FES at small k and for $N = 4096$; see Eq. (2). One should remark that the data collapse follows from measuring the time in units of t_s, Eq. (7), which incorporates all the different values of the initial conditions and the parameters of the Hamiltonian.

observed resembles the one of turbulence in fluids [25], with an inertial range $[k_0, k_c]$ over which the FES displays a power-law decay. However, in absence of energy injection and dissipation, we are here in the presence of a transient turbulence phenomenon. Moreover, it must be stressed that the values of the exponent 8/3 at t_s and 2 at later times are clear signatures of an evolution guided by the *integrable* Burgers dynamics [26]. Finally, like in fluid turbulence, we observe an exponential decay of the FES beyond the inertial range, i.e., for values of $k > k_c$. In fluids this is due to a small scale balance between nonlinearity and dissipation [25], whereas in our case the role of dissipation is played by dispersion. In addition, as for decaying turbulence in fluids, after the transient turbulence regime we observe that the exponential falloff disappears and the FES becomes flat, eventually leading to energy equipartition. The phenomenology treated here does not fall into the range of applicability of the so-called (weak) wave turbulence [27,28], which would require an unfitting assumption of weak nonlinearity.

Model, initial conditions, and continuum approximation.—All the details of the following analytical derivation are reported in the Supplemental Material [29] (see Ref. [32] for the mathematical framework).

For the FPUT model Eq. (1) we choose periodic boundary conditions: $q_N = q_0$ and $p_N = p_0$. Defining the Fourier coefficient $\hat{q}_k = (1/\sqrt{N})\sum_{j=1}^N q_j e^{\imath 2\pi kj/N}$ of the displacements q_j, and similarly for the momenta p_j, the energy of the linearized system is consequently written as

$$H_{\rm lin} = \sum_{k=1}^N E_k, \qquad E_k \coloneqq \frac{|\hat{p}_k|^2}{2} + \frac{\omega_k^2|\hat{q}_k|^2}{2}, \tag{3}$$

where $\omega_k = 2\sin(\pi k/N)$ and E_k is the energy of mode k.

We consider the two-parameter family of initial data:

$$q_j(0) = A\cos\varphi \sin\left(\frac{2\pi j}{N}\right), \tag{4a}$$

$$p_j(0) = \omega_1 A \sin\varphi \cos\left(\frac{2\pi j}{N}\right), \tag{4b}$$

for $j = 1, \ldots, N$. Here, $A > 0$ and $0 \leq \varphi \leq \pi/2$ are the amplitude and the phase of the initial excitation. Varying the phase from $\varphi = 0$ to $\varphi = \pi/2$, we tune the kinetic energy of the initial condition (4). The value $\varphi = \pi/4$ corresponds to a left traveling wave excitation (TWE), around which we explore a large neighborhood. The specific energy $\varepsilon = E/N$ can be written in terms of A and φ, for large N, as

$$\varepsilon = a^2 + \frac{3\beta}{2}(a\cos\varphi)^4, \qquad a = \frac{\pi A}{N}. \tag{5}$$

In order to study the evolution of the initial condition (4) in the continuum limit $N \to \infty$, at fixed small a, we first introduce two fields $Q(x,\tau)$ and $P(x,\tau)$ of spatial period one, such that $q_j(t) = NQ(j/N, t/N)$, $p_j(t) = P(j/N, t/N)$.

In order to separate the right from the left motion at zero order in the small parameter a, we then introduce the "left" and "right" fields $L = (Q_x + P)/(a\sqrt{2})$, $R = (Q_x - P)/(a\sqrt{2})$, where partial derivatives are denoted by subscripts.

The evolution equations in the continuum limit read $L_\tau = L_x + O(a)$, $R_\tau = -R_x + O(a)$, which in the harmonic limit $a \to 0$ uncouple into the left and right translations of the initial conditions $L_0(x)$ and $R_0(x)$. It follows from Eq. (4) that L_0 has maximal amplitude for $\varphi = \pi/4$, when $R_0 = 0$, which defines the left TWE. The equations of motion display the symmetry $\varphi \to -\varphi$, $L \to R$.

Since the equations for L and R are nonlinearly coupled for any $a > 0$, we build up a transformation $\mathcal{C}_a : (L, R) \mapsto (\lambda, \rho)$ of the fields matching the identity for $a \to 0$ and such that the evolution equations of the new fields λ and ρ turn out to be decoupled to order a^2 included. A rather long computation yields [29]

$$\lambda_\tau = \Phi(\lambda)\lambda_x, \qquad \rho_\tau = -\Phi(\rho)\rho_x, \tag{6a}$$

$$\Phi(\lambda) = \frac{a\alpha}{\sqrt{2}}\lambda + \frac{3a^2\alpha^2}{4}\left(\frac{\beta}{\alpha^2} - \frac{1}{2}\right)\lambda^2, \tag{6b}$$

with initial conditions $(\lambda_0, \rho_0) = \mathcal{C}_a(L_0, R_0)$.

Because of the form of the nonlinearity, Eqs. (6) reduce to a pair of Burgers equations if $\beta = (\alpha^2/2)$ or, otherwise, to a pair of generalized Burgers equations.

Shock time and universal FES.—The equations of motion (6a) for the left and right fields $\lambda(x,\tau)$ and $\rho(x,\tau)$ have the form of two uncoupled inviscid, generalized Burgers equations. Their solution exists in a finite time interval $[0, \tau_s[$, where τ_s is the shock time [29].

Taking into account the time rescaling $t_s = N\tau_s$, we obtain the following expression for the FPUT shock time t_s:

$$t_s = \left(\frac{N}{2\pi\sqrt{2}a\alpha}\right)\frac{F(\mu)}{\cos\theta}, \tag{7}$$

where the function $F(\mu)$ and the auxiliary parameter μ are given by

$$F(\mu) = \sqrt{\frac{32\mu^2}{\sqrt{1+32\mu^2} - 1 + 16\mu^2}\frac{4}{\sqrt{1+32\mu^2}+3}}, \tag{8}$$

$$\mu = \frac{a\alpha}{2\sqrt{2}}\cos\theta\left[\tan^2\theta - 4\tan\theta + 6\left(\frac{\beta}{\alpha^2} - \frac{1}{2}\right)\right]. \tag{9}$$

Equation (7) is valid for a small enough and $-\pi/4 \leq \theta \leq \pi/4$, where $\theta = \varphi - \pi/4$.

In order to estimate the FES of the FPUT model at the shock time t_s, we generalize the procedure of Ref. [26] and compute the exact solution of Eq. (6) in Fourier space,

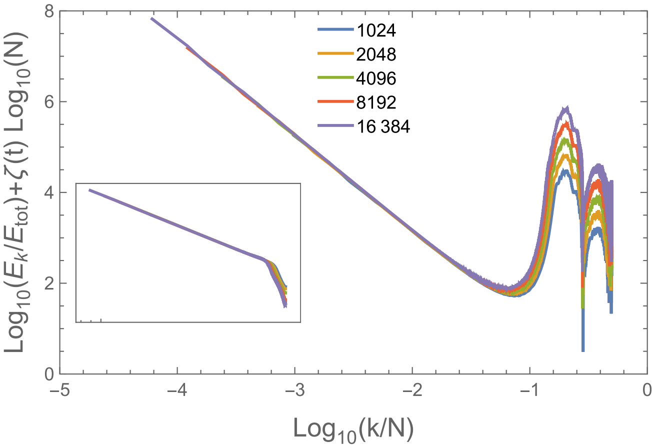

FIG. 4. FES versus k/N, left TWE at $4t_s$, $\alpha = 1$, $\beta = 1/2$, $\varepsilon = 0.05$, and different values of N. Inset: the same at t_s.

$$\hat{\lambda}_k(\tau) = \frac{1}{\imath 2\pi k}\oint \lambda_0'(x) e^{-\imath 2\pi k(x-\tau\Phi(\lambda_0(x)))}dx, \qquad (10)$$

and the analogous expression for $\hat{\rho}_k(\tau)$. Then, for a general class of initial conditions the method of (degenerate) stationary phase applied to the integral (10) yields $|\hat{\lambda}_k(\tau_s)|^2 \sim Ck^{-8/3}$ for large k, where C is an explicit constant independent of k. It also turns out that $|\hat{\rho}_k(\tau_s)|^2$ is smaller than $|\hat{\lambda}_k(\tau_s)|^2$, the smaller the closer θ is to $\pi/4$, equality holding for $\theta = \pm\pi/4$. Taking into account the relation

$$E_k(t_s) \propto |\hat{\lambda}_k(\tau_s)|^2 + |\hat{\rho}_k(\tau_s)|^2, \qquad (11)$$

we derive the normalized FES of the FPUT system as

$$\frac{E_k(t_s)}{\sum_k E_k(t_s)} = (0.7787\ldots)k^{-8/3}. \qquad (12)$$

Note that the shock time t_s incorporates all the dependencies of the FES on the parameters of the system and of the initial conditions, so that the spectrum (12) is indeed *universal*.

We have performed massive numerical simulations [34] of the FPUT system Eqs. (1)–(4). The FES at the shock time, Eq. (7), is displayed in Fig. 2 for different initial conditions. The universal FES (12) works over 6–7 orders of magnitude in mode energy, and the scenario is robust over 3 orders of magnitudes in specific energy. Figure 2 also shows the presence of an exponential cutoff beyond k_c, consistently with the theory of Ref. [15]. We have verified that $k_c/N \propto \varepsilon^{1/4}$, in agreement with Refs. [17,36], so that the scaling region in k is extensive, as shown in Fig. 4.

Beyond the shock time.—The solution of the generalized Burgers equations (6) no longer exists for times $\tau > \tau_s = t_s/N$, due to a local divergence of the derivatives of the fields. Such a "gradient catastrophe" implies a transfer of energy to the highest Fourier modes of wavelength $\sim 1/N$, so that a global continuum limit no longer holds after the shock. For a correct continuum description of the shock region, higher-order derivatives of the fields must be taken into account, which replaces the Burgers equations with a pair of KdV equations [32,37–39]. However, far from the shock region, the Burgers equation still describes the FPUT dynamics. Indeed, let us consider the left TWE $\lambda(x,0) = 2\cos(2\pi x)$ with $\beta = 1/2$ in order to eliminate the quadratic term in a in Eq. (6b). In this case system (6) yields the Burgers equation $\lambda_\tau = (a\alpha/\sqrt{2})\lambda\lambda_x$, whose solution is obtained from the implicit equation $\lambda = 2\cos(2\pi(x + (a\alpha/\sqrt{2})\lambda\tau))$. The initial cosine is progressively deformed into a sawtooth profile $\sigma(x)$ with the discontinuity at $x = 3/4$ (the point in which the initial cosine vanishes and the profile has positive derivative) and slope -4. Performing a Fourier transform one finds that

$$\sigma(x) = \sum_{k\neq 0}\frac{2}{\imath\pi k}e^{\imath 2\pi k(x+1/4)}. \qquad (13)$$

It can be shown that the time needed for the position of the maximum of the initial cosine to reach the node at $x = 3/4$ is $(\pi/2)\tau_s$, thus larger than the shock time τ_s. At the shock time τ_s the spatial derivative of λ becomes infinite in the Burgers equation, huge but finite on the lattice due to dispersion. The formation of the sawtooth profile then follows in time the creation of the shock. Heuristically, after this formation, one can decompose the wave profile as $\lambda(x,\tau) = \sigma(x) + r(x,\tau)$, where the deviation r with respect to the sawtooth profile (13) is smooth. The Fourier coefficients of $\sigma(x)$ decay as $1/k$, while those of the smooth deviation r can be shown to decay faster [40]. Therefore, the FES of λ is dominated by $|\hat{\sigma}_k|^2 \propto k^{-2}$. This heuristic argument can be verified in numerical experiments by measuring the slope of the FES after the shock time. The time evolution of the slope is shown in Fig. 3: one observes an extended time domain (approximately from two to four shock times) where the slope remains close to -2. The relevance of the scaling exponent 2 for Burgers turbulence was already established in Ref. [26] and further analyzed in Ref. [41]. Although the numerical determination of the slope for later times becomes much harder, it can be seen that it eventually increases, detecting a trend to equipartition, which corresponds to a vanishing slope and the disappearance of the exponential falloff. It is also important to highlight the data "collapse," which is a consequence of measuring time in units of the shock time, t_s Eq. (7). In the inset of Fig. 2 we display the FES at $4t_s$ in order to confirm that $\zeta = 2$. We observe the additional presence of a peak at large k. We plot in log-log scale the energy spectrum versus k adjusting a line with slope -2 on the experimental data.

In a statistical mechanical perspective, the FES versus k/N is reported in Fig. 4. The proportionality to N of the power-law window is evident, which implies that Burgers turbulence is a relevant phenomenon in the thermodynamic limit of the FPUT system.

In order to explain the presence of the peaks in the FES of Fig. 2, we go back to the analysis of Fig. 1. We display there the numerical profiles of the left TWE, i.e., $(q_{j+1} - q_j + p_j)/(\sqrt{2}a)$ versus j, up to a suitable Galilean translation [29], for three different times. We clearly observe the formation of the sawtooth profile, and the fast oscillations near the discontinuity of the profile. These oscillations have been studied by various authors [24] in the context of the nondispersive limit of the KdV equation. In our approach, this oscillatory part of the profile is included in the smooth deviation r from the sawtooth σ. We think that these oscillations are the main feature of the spatial profile which determines the observed peak in the FES at large k.

Short-wavelength oscillations are found also in the Galerkin-truncated Burgers equation. These oscillations, called "tygers" (see, e.g., Ref. [42]), are however of different nature with respect to the ones observed in FPUT: tygers are due to the Galerkin truncation, while the ones we observe in the FPUT are due to the small dispersion term of the approximating KdV dynamics. Nevertheless, phenomena similar to the ones that give rise to the tygers, such as tail resonances in the energy spectrum [43], may be an explanation of these short-wavelength oscillations. A possible connection between tygers and our oscillations could be the subject of a separate study.

Conclusions.—In this Letter we have shown that the Fourier energy spectrum of the FPUT chain displays, in a wide range of specific energies, an inertial range characterized by a power-law scaling. The values of the time-dependent exponent and the timescales involved are theoretically predicted by performing a nontrivial continuum limit of the lattice model. This procedure allows us to describe the FPUT dynamics with a pair of generalized, inviscid Burgers equations. The power-law exponent of the Fourier energy spectrum of the chain takes the value $8/3$ at the shock time and then stabilizes around 2 before the system eventually relaxes to equipartition. These results hold for a much larger class of initial conditions than the one discussed in this Letter, as stated below Eq. (10). In fact, the mathematical results on the asymptotics of the spectrum proven in the Supplemental Material [29] are valid for a generic superposition of Fourier modes. Our result provides a direct relation between the FPUT dynamics and Burgers turbulence. Besides considerably expanding the phenomenology of the FPUT chain with an impact on the problem of relaxation to equilibrium, we believe that our results are relevant for the experimental investigations of physical systems described by the FPUT dynamics, i.e., phononic, photonic, or cold atomic systems at energies higher than those at which the FPUT "recurrence" phenomenon has already been observed [9].

This work was partially supported by GNFM (INdAM) the Italian national group for Mathematical Physics, the MIUR PRIN 2017 project MaQuMA No. 2017ASFLJR, and the MIUR PRIN 2017 project "Coarse-grained description for non-equilibrium systems and transport phenomena (CO-NEST)" No. 201798CZL. M. G. and A. P. thank SISSA for hospitality.

[*]matteo.gallone@sissa.it
[†]matteo.marian@studenti.units.it
[‡]ponno@math.unipd.it
[§]ruffo@sissa.it

[1] R. Balescu, *Statistical Dynamics: Matter Out of Equilibrium* (Imperial College Press, London, 1997).
[2] E. Fermi, J. Pasta, and S. Ulam, Studies of non linear problems, Los-Alamos Internal Report, Document LA-1940 (1955), in Enrico Fermi Collected Papers (The University of Chicago Press, Chicago, and Accademia Nazionale dei Lincei, Roma, 1965), Vol. **II**, pp. 977–988 (also reproduced in Ref. [3]).
[3] G. Gallavotti, *The Fermi-Pasta-Ulam Problem: A Status Report*, Lecture Notes in Physics (Springer, New York, 2008).
[4] N. J. Zabusky and M. D. Kruskal, Phys. Rev. Lett. **15**, 240 (1965).
[5] A. N. Kolmogorov, Dokl. Akad. Nauk SSSR **98**, 527 (1954); V. I. Arnold, Usp. Mat. Nauk **18**, 13 (1963); Russ. Math. Surv. **18**, 9 (1963); J. Moser, Nach. Akad. Wiss. Göttingen. Math. Phys. Kl. II **1**, 1 (1962).
[6] F. M. Izrailev and B. V. Chirikov, Dokl. Akad. Nauk SSSR **166**, 57 (1966) Sov. Phys. Dokl. **11**, 30 (1966).
[7] D. Midtvedt, A. Croy, A. Isacsson, Z. Qi, and H. S. Park, Phys. Rev. Lett. **112**, 145503 (2014).
[8] L. S. Cao, D. X. Qi, R. W. Peng, M. Wang, and P. Schmelcher, Phys. Rev. Lett. **112**, 075505 (2014).
[9] D. Pierangeli, M. Flammini, L. Zhang, G. Marcucci, A. J. Agranat, P. G. Grinevich, P. M. Santini, C. Conti, and E. DelRe, Phys. Rev. X **8**, 041017 (2018).
[10] T. Kinoshita, T. Wenger, and D. S. Weiss, Nature **440**, 900 (2006).
[11] P. Villain and M. Lewenstein, Phys. Rev. A **62**, 043601 (2000).
[12] I. Danshita, R. Hipolito, V. Oganesyan, and A. Polkovnikov, Prog. Theor. Exp. Phys. **2014**, 43I03 (2014).
[13] M. Hénon, Phys. Rev. B **9**, 1921 (1974).
[14] T. Goldfriend and J. Kurchan, Phys. Rev. E **99**, 022146 (2019); D. Barbier, L. Cugliandolo, G. Lozano, and N. Nessi, Europhys. Lett. **132**, 50002 (2020).
[15] F. Fucito, F. Marchesoni, E. Marinari, G. Parisi, L. Peliti, S. Ruffo, and A. Vulpiani, J. Phys. (Paris) **43**, 707 (1982).
[16] R. Livi, M. Pettini, S. Ruffo, M. Sparpaglione, and A. Vulpiani, Phys. Rev. A **28**, 3544 (1983).
[17] D. L. Shepelyansky, Nonlinearity **10**, 1331 (1997).
[18] A. Ponno, Europhys. Lett. **64**, 606 (2003).
[19] L. Casetti, M. Cerruti-Sola, M. Pettini, and E. G. D. Cohen, Phys. Rev. E **55**, 6566 (1997); J. De Luca, A. J. Lichtenberg, and S. Ruffo, Phys. Rev. E **60**, 3781 (1999).
[20] G. Benettin and A. Ponno, J. Stat. Phys. **144**, 793 (2011).
[21] R. Livi, M. Pettini, S. Ruffo, M. Sparpaglione, and A. Vulpiani, Phys. Rev. A **31**, 1039 (1985).
[22] G. Ooms and B. J. Boersma, Chaos **18**, 043124 (2008).

[23] P. Poggi, S. Ruffo, and H. Kantz, Phys. Rev. E **52**, 307 (1995).

[24] P. D. Lax, C. D. Levermore, and S. Venakides, in *Important Developments in Soliton Theory*, edited by A. S. Fokas and V. E. Zakharov, Springer Series in Nonlinear Dynamics (Springer, Berlin, 1993).

[25] U. Frisch and G. Parisi, Fully developed turbulence and intermittency, in edited by M. Ghil, R. Benzi, and G. Parisi, *Turbulence and Predictability in Geophysical Fluid Dynamics and Climate Dynamics, Proceeding of the International School of Physics "E. Fermi", North-Holland, New York* (1985), pp. 71–88.

[26] J. D. Fournier and U. Frisch, J. Mech. Theor. Appl. **2**, 699 (1983).

[27] M. Onorato, L. Vozella, D. Proment, and Y. V. Lvov, Proc. Natl. Acad. Sci. U.S.A. **112**, 4208 (2015).

[28] Y. V. L'vov and M. Onorato, Phys. Rev. Lett. **120**, 144301 (2018).

[29] See Supplemental Material at http://link.aps.org/supplemental/10.1103/PhysRevLett.129.114101 for all the details of the computations, which includes Refs. [30–33].

[30] I. M. Gelfand and S. V. Fomin, *Calculus of Variations* (Dover, New York, 2000).

[31] J. E. Marsden and T. S. Ratiu, *Introduction to Mechanics and Symmetry*, 2nd ed. (Springer, New York, 1999).

[32] M. Gallone and A. Ponno, arXiv:2202.13454.

[33] A. Erdélyi, *Asymptotic Expansions* (Dover, New York, 1956).

[34] For the numerical study we used a sixth-order Yoshida algorithm [35] with time step $\Delta t = 0.001$ and initial condition given by Eq. (4). We fixed $\alpha = 1$ without any loss of generality, and varied β around $\alpha^2/2$, $\theta = \varphi - \pi/4$ in the interval $[-\pi/4, \pi/4]$, and $\varepsilon = E/N$ in the range 0.0005–0.1. Concerning the size of the system, we considered the values $N = 2^n$, with n ranging from 10 to 14. To compare data with different number of particles, we kept constant the specific energy ε assigning the parameter A properly.

[35] H. Yoshida, Phys. Lett. **150A**, 262 (1990).

[36] L. Berchialla, L. Galgani, and A. Giorgilli, Discrete Cont. Dyn. Sys. A **11**, 855 (2004).

[37] A. Ponno and D. Bambusi, Chaos **15**, 015107 (2005).

[38] D. Bambusi and A. Ponno, Commun. Math. Phys. **264**, 539 (2006).

[39] M. Gallone, A. Ponno, and B. Rink, J. Phys. A **54**, 305701 (2021).

[40] For $f \in C^\infty[0,1]$, f periodic, all the derivatives are finite. Since $d^n f(x)/dx^n = \sum_k (\imath 2\pi k)^n \hat{f}_k e^{\imath 2\pi kx}$, one also has $\hat{f}_k = (1/(\imath 2\pi k)^n) \int_0^1 e^{-\imath 2\pi kx}[d^n f(x)/dx^n]dx$ implying that $\hat{f}_k$ decays faster than any power in k.

[41] S. Kida, J. Fluid Mech. **93**, 337 (1979).

[42] S. S. Ray, U. Frisch, S. Nazarenko, and T. Matsumoto, Phys. Rev. E **84**, 016301 (2011).

[43] T. Penati and S. Flach, Chaos **17**, 023102 (2007).